Structural Monitoring and Maintenance, *Vol. 11, No. 4 (2024) 349-367*
https://doi.org/10.12989/smm.2024.11.4.349

Delamination analysis of a multilayered beam structure under bending at a constant velocity

Victor I. Rizov*

Department of Technical Mechanics, University of Architecture, Civil Engineering and Geodesy, 1 Chr. Smirnensky blvd., 1046 – Sofia, Bulgaria

(*Received October 17, 2024, Revised December 7, 2024, Accepted December 17, 2024*)

Abstract. Delamination cracks are detected often in multilayered beam structures during lifetime. This fact raises concerns about serviceability of multilayered structures. Apparently, there is a need for tools to adequately predict whether further functioning of these structures is safe. Developing of such tool is subject of this work. In particular, the work is concerned with the problem of delamination analysis of a multilayered beam structure subjected to bending at a constant velocity (the angle of rotation of the free end of the lower arm of the delamination crack varies with time at a constant velocity). The layers of the beam are made of non-linear elastic structural materials that exhibit smooth inhomogeneity along the thickness. Therefore, the material parameters of the non-linear constitutive law are continuous function of the transversal coordinate, z. The method of the integral J is used for analyzing the delamination behavior of the beam. The analysis takes into account the bending velocity. A check-up of the analysis is performed by deriving the strain energy release rate (SERR). The analysis is applied for determining the safe velocity of the angle of rotation. The safe delaminaton length and the time of safe functioning of the beam structure are determined too. The effect of additional support introduced in the beam on the time of safe functioning is also evaluated.

Keywords: analysis; delamination; material inhomogeneity; multilayered structure; safety; serviceability

1. Introduction

There is a need of using of more efficient structural materials in various applications in modern engineering. The reason for this is the constant striving for reducing the weight and improving the performance of engineering structures and facilities. The weight reduction, however, should not threaten the safety and reliability of structures and to shorten their lifetime. To meet these needs nowadays the scientists around the world are developing different innovative structural materials.

A large number of publications related to the subject of development and application of new materials can be found in the specialized literature during the last decades. One of the efficient and very promising class of novel materials are the functionally graded engineering materials (Akbaş *et al*. 2021, Butcher *et al*. 1999, Gasik 2010, Han *et al*. 2001, Hedia *et al*. 2014). In fact, they represent innovative composites with continuously changing mechanical properties along chosen directions. The basic idea of the functionally graded materials is that the distribution of their

*Corresponding author, Professor, E-mail: V_RIZOV_FHE@UACG.BG

 ISSN: 2288-6605 (Print), 2288-6613 (Online)

properties can be tailored during manufacturing process so as to achieve significant improvement of the performance of structures and facilities (Civalek *et al.* 2021, Faleh *et al.* 1999, Hirai and Chen 1999, Nemat-Allal *et al.* 2011, Raad *et al.* 2019, Ridha *et al.* 2019, Saiyathibrahim *et al.* 2016, Shrikantha and Gangadharan 2014, Van Thinh and Van Tung 2023). The excellent properties of these materials are the most important premise for their increasing use in a variety of engineering applications (Dastjerdi *et al.* 2020, Mahamood and Akinlabi 2017, Markworth *et al.* 1995, Miyamoto *et al.* 1999, Rizov 2014, Rizov 2020, Rizov and Altenbach 2022, Dastjerdi *et al.* 2022, Dastjerdi *et al.* 2023, Long and Van Tung 2023, Van Thinh and Van Tung 2023, Wu *et al*. 2014). That is why the functionally graded materials and structures have experienced a very intensive development recently. Studying the behavior of these materials under various loadings is very important for guaranteeing the safety of engineering structures. In this context, interesting analyses of the response of functionally graded beams and microbeams under moving loads are presented in (Fenjan *et al*. 2020, Akbaş *et al*. 2022). Another widespread class of modern inhomogeneous structural materials with very good perspectives is the multilayered materials (Dolgov 2002, Dolgov 2005, Dolgov 2016, Dowling, 2013, Rizov 2020, Rizov 2024, Nguyen *et al*. 2020). In principle, a multilayered material represents a system of layers of different materials assembled together in an appropriate way with goal of achieving a significant improvement of the quality and performance of a structure for particular conditions of use. For instance, a multilayered system may be designed so as to achieve a considerable reduction of the weight of the structure. It should be noted further that layers can be inhomogeneous (functionally graded) (Cinefra and Soave 2011, Kushnir *et al*. 2022, Tokovyy 2023). Therefore, analyzing of inhomogeneous multilayered systems can be regarded as an important task.

Although inhomogeneous multilayered engineering materials and their application in load-bearing structures has been a field of increasing research activities recently, there are some aspects of their behavior which need more efforts for clarification. For example, it is now widely recognized that safety and reliability of multilayered structures is related in a high degree to their delamination behavior (Dolgov 2005, Dolgov 2016, Dowling 2013, Rizov 2023, Rizov 2024). Therefore, the use of multilayered materials in a variety of practical applications is strongly influenced by the progress in studying the delamination (Almeida *et al.* 2016, Boyano *et al.* 2021, Dinesh Babu *et al.* 2023, Hofinger *et al.* 1998, Huang and Bobyr 2023, Köllner *et al*. 2026, Rzeczkowski 2021, Sridhar *et al.* 2002, Treber *et al*. 2017). The delamination fracture is studied across beam specimens of fiber reinforced epoxy laminates that are used for manufacturing of turbine blades (Boyano *et al.* 2021). Delamination in curved laminates strengthened by different types of reinforcement under four-point bending loading conditions is examined and analyzed (Dinesh Babu *et al.* 2023). The SERR for delamination cracks in thin layers bonded to a substrate is examined (Hofinger *et al.* 1998). The reasons for delamination in the process of manufacturing and application and its influence on the load-bearing capacity of different structural members made of layered composite materials are discussed and systematized (Huang and Bobyr 2023). An analytical model for dealing with buckling and postbuckling behavior of delaminated composite structures by using a potential energy approach is presented (Köllner *et al*. 2026). Exploring of delamination fracture toughness of laminates by using beam specimens under four-point-bending loading conditions is presented in (Rzeczkowski 2021). Beam theory formulations are used for studying dynamic delamination fracture in through-thickness reinforced composite structures (Sridhar *et al.* 2002). Results of exploring the delamination fracture toughness of laminates are reported in (Treber *et al*. 2017). The development of advanced approaches for carrying-out high-quality analyses of different delamination problems will stimulate the application of the

multilayered material and structures in many areas of the up-to-date engineering. However, delamination of multilayered structures is a complex problem for analysis and clarification. The reason is that there are many factors like the number of layers in the structure, type of the external influence applied on the structure, mechanical behavior of the structure, number and location of the supports, etc. which may influence delamination behavior of a particular multilayered structure in one or other way.

Delamination cracks are detected often in multilayered beam structures in service. Such cracks raise well-founded concerns about further safe functioning of the structures. The current work has for its purpose developing of a delamination analysis that can be applied for checking if further functioning of multilayered beams in which a delamination crack is detected is safe. The analysis is based on the J integral. The beam layers are inhomogeneous and have non-linear elastic behavior. Perfect adhesion between layers of the beam is assumed. The angle of rotation of the free end of the lower arm of the delamination crack in the beam varies with time at a constant velocity (this is the only external influence applied on the beam). The proposed analysis takes into account influencing factors like number of layers (the beam analyzed has an arbitrary number of inhomogeneous layers), number and location of supports, non-linear elastic behavior of the inhomogeneous multilayered beam structure, and the velocity of angle of rotation (actually, taking into account these factors is the novelty of the current work).

The current work is organized as follows. First, an analysis of the delamination is performed by using the J integral. This analysis accounts for the above mentioned influencing factors. Then, a check-up of the analysis is done by deriving the SERR. Finally, the analysis is applied for determination of the safe velocity of the angle of rotation. The safe delamination length and the time of safe functioning of the beam are determined too. The effect of additional support introduced in the beam on the time of safe functioning is also evaluated.

2. Theoretical analysis

The delamination problem that is addressed in this work is presented in Fig. 1. As seen in Fig. 1, the multilayered beam structure is assumed to be delaminated in portion, B_1B_2. The end, B_3, of the beam is motionless (rigidly fixed). It is assumed that the only external influence applied on the beam is the rotation of the end, H_1H_2, of the lower arm of the delamination crack. The angle of this rotation is denoted by φ as seen in Fig. 1. This angle varies with time, t, as defined by Eq. (1).

$$\varphi = v_\varphi t\,, \tag{1}$$

where v_φ is the velocity of ϕ. Since ϕ is directed anticlockwise, the upper arm of the delamination crack is free of stresses.

It is assumed further that the beam behaves as a non-linear elastic body. This behavior is treated by the non-linear constitutive law defined by Eq. (2) (Tsankov 1996).

$$\sigma_i = E_i \varepsilon^{n_i} \left(1 + L_i \frac{\dot{\varepsilon}}{\dot{\varepsilon}_0} \right) \tag{2}$$

$$i = 1, 2, ..., m \tag{3}$$

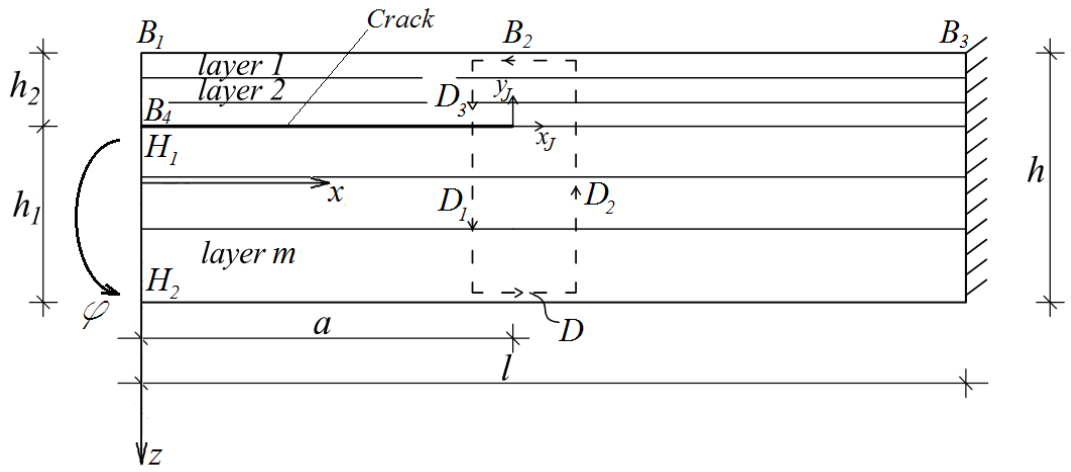

Fig. 1 The delamination problem addressed in the present work

where σ_i is the stress, ε is the strain, E_i, n_i, L_i and $\dot{\varepsilon}_0$ are parameters in the context of the non-linear elastic behavior, m is the number of layers in the beam (the subscript i in (2) refer to the i-the layer of the beam). The dot in Eq. (2) represents the time derivative.

The parameters, E_i, n_i and L_i, change along the thickness of each layer since the layers are inhomogeneous. The change of E_i, n_i and L_i is defined by Eqs. (4)-(6), respectively.

$$E_i = E_{igr} + \frac{E_{idl} - E_{igr}}{(z_{i+1} - z_i)^{\lambda}} z^{\lambda} \tag{4}$$

$$n_i = n_{igr} + \frac{n_{idl} - n_{igr}}{(z_{i+1} - z_i)^{\mu}} z^{\mu} \tag{5}$$

$$L_i = L_{igr} + \frac{L_{idl} - L_{igr}}{(z_{i+1} - z_i)^{\rho}} z^{\rho} \tag{6}$$

$$z_i \le z \le z_{i+1} \tag{7}$$

where the subscripts, igr and idl, refer to the upper and lower surface of the layer, z is the vertical axes of the beam cross-section as illustrated in Fig. 2, z_i and z_{i+1} are the coordinates of the upper and lower surface of the layer as seen in Fig. 2, λ, μ and ρ are parameters.

The theoretical approach applied for studying the delamination in this work is based upon the integral J (Broek 1986). The analytical expression of J is presented by Eq. (8).

$$J = \int \left[u_0 \cos\alpha - \left(p_{xa} \frac{\partial u}{\partial x_a} + p_{ya} \frac{\partial v}{\partial x_a} \right) \right] ds \tag{8}$$

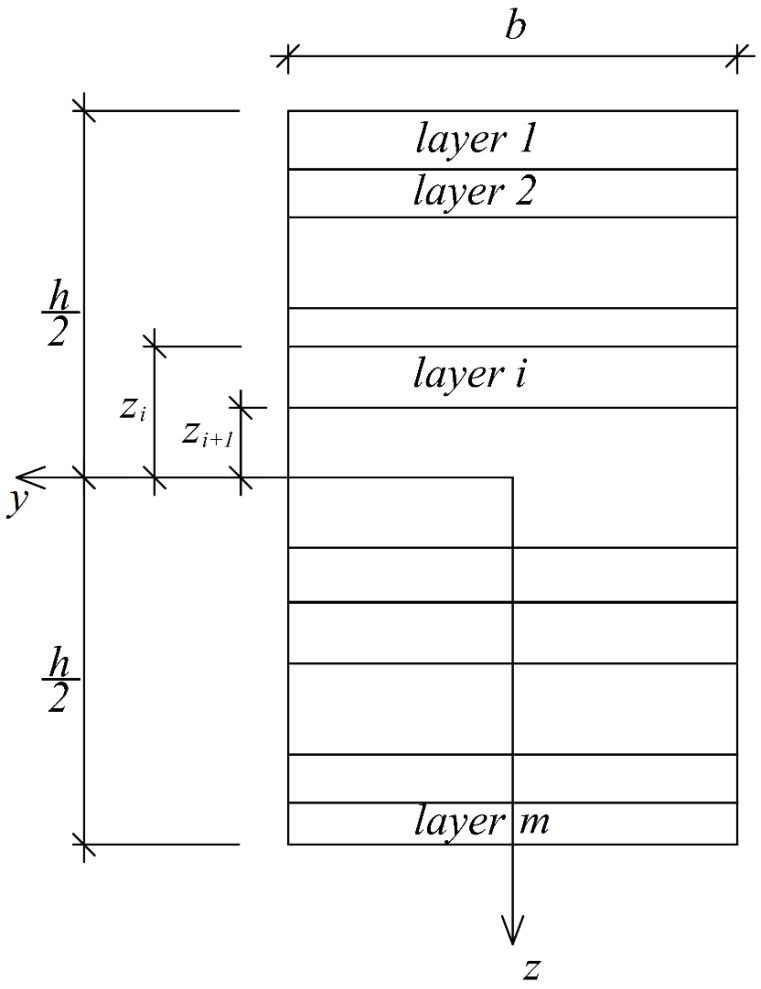

Fig. 2 Beam cross-section

The quantities involved in Eq. (8) are defined as follows: u_0 is density of the strain energy, α is the angle between the outward normal of the integration contour and the x_J-axis, p_{xa} and p_{ya} are the stresses acting on the integration contour and directed along axes, x_J and y_J, respectively, u and v are the displacements of the integration contour along x_J and y_J, respectively.

The integration contour, D, that is used here has three parts, D_1, D_2 and D_3, as seen in Fig. 1. As mentioned previously, the upper arm of the delamination crack is free of stresses. Therefore, the value of the integral *J* is zero in part, D_3, of the integration contour. That is why, the solution of *J* is

$$J_D = J_{D1} + J_{D2} \tag{9}$$

where the subscripts, D_1 and D_2, refer to parts, D_1 and D_2, of the integration contour, respectively. Since the beam is multilayered, J_{D1} and J_{D2} are written as given below

$$J_{D1}=\sum_{i=1}^{i=m_{lwd}}\int\left[u_{0D1i}\cos\alpha_{D1}-\left(p_{xJD1i}\frac{\partial u_{D1}}{\partial x_J}+p_{yJD1i}\frac{\partial v_{D1}}{\partial x_J}\right)\right]ds_1 \tag{10}$$

$$J_{D2}=\sum_{i=1}^{i=m}\int\left[u_{0D2i}\cos\alpha_{D2}-\left(p_{xJD2i}\frac{\partial u_{D2}}{\partial x_i}+p_{yJD2i}\frac{\partial v_{D2}}{\partial x_J}\right)\right]ds_2 \tag{11}$$

where m_{lwd} is the number of layers in the lower arm of the delamination crack, the subscript, i, refer to the i-th layer. It is assumed that the angles of rotation of the beam sections in each layer are equal, since long beams, i.e. beams which have high length to thickness ratio are treated in this paper (on this base, we assume linear distribution of longitudinal displacements along the thickness of the beam).

First, the quantities involved in (10) are derived. This is done with the help of the Eqs. (12)-(18).

$$u_{0D1i}=\int\sigma_{lwdi}d\varepsilon_{lwd} \tag{12}$$

where σ_{lwdi} is the stress in a layer of the lower arm of the delamination crack, ε_{lwd} is the strain in the same delamination crack arm. The stress, σ_{lwdi}, is related to the strain, ε_{lwd}, via the law (2). For this purpose, ε is replaced by ε_{lwd} in (2).

The other quantities in (10) are expressed as given below.

$$\cos\alpha_{D1}=-1 \tag{13}$$

$$p_{xJD1i}=-\sigma_{lwdi} \tag{14}$$

$$\frac{\partial u_{D1}}{\partial x_J}=\varepsilon_{lwd} \tag{15}$$

$$p_{yJD1i}=0 \tag{16}$$

$$ds_1=dz_1 \tag{17}$$

Where

$$-\frac{h_1}{2}\le z_1\le\frac{h_1}{2} \tag{18}$$

$\cos\alpha_{D1}$ is equal to -1 since the angle, α_{D1}, between the outward normal vector towards part, D_1, of the contour of integration and the axis, x_J, is 180^0. Here, z_1 and h_1 are the vertical axis and the thickness of the cross-section of the lower arm of the delamination crack, respectively (Fig. 3). Next, the quantities involved in (11) are obtained. Eqs. (19) – (24) are used.

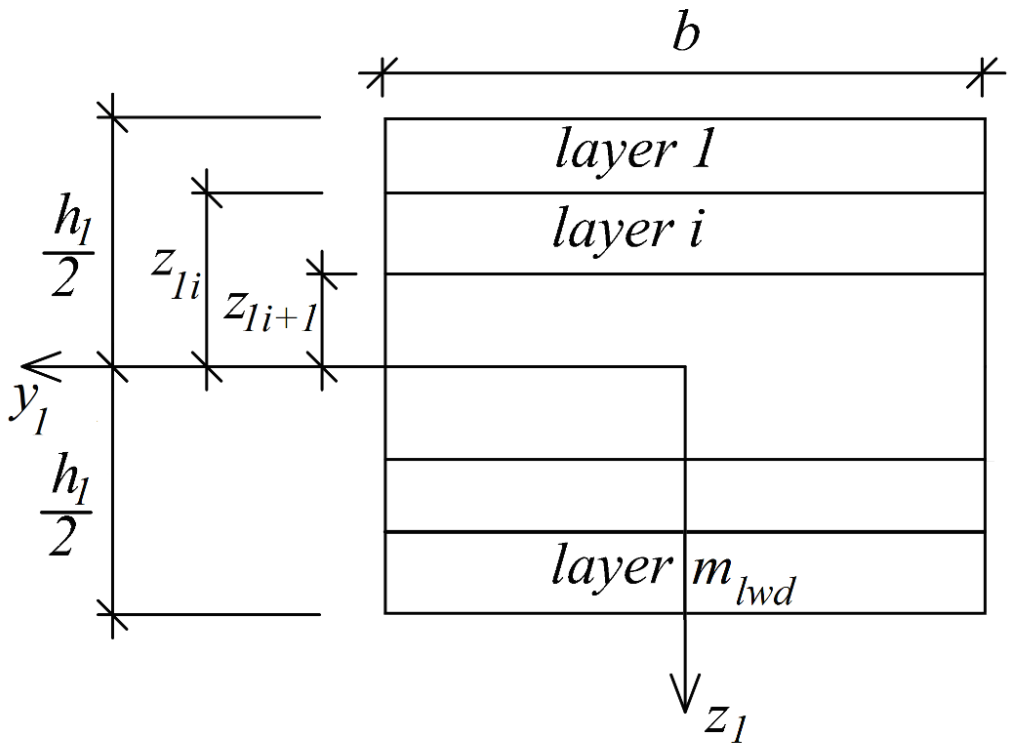

Fig. 3 Cross-section of the delamination crack lower arm

$$u_{0D2i} = \int \sigma_i d\varepsilon \ , \tag{19}$$

where the stress, σ_i, in a layer of the intact portion of the beam is related to the strain, ε, via the law (2).

The other quantities in (11) are derived as given below.

$$\cos\alpha_{D2} = 1 \tag{20}$$

$$p_{xJD1i} = \sigma_i \tag{21}$$

$$\frac{\partial u_{D2}}{\partial x_J} = \varepsilon \tag{22}$$

$$p_{yJD2} = 0 \tag{23}$$

$$ds_2 = -dz_2 \tag{24}$$

where z_2 is the vertical axis of the beam cross-section. $\cos\alpha_{D2}$ is equal to 1 since the angle, α_{D2}, between the outward normal vector towards part, D_2, of the contour of integration and the

axis, x_J, is zero.

The quantities which are involved in Eqs. (12)-(24) are analyzed by the approach presented below.

First, the angle of rotation, φ, is expressed via the longitudinal displacements, u_{H1} and u_{H2}, of points, H_1 and H_2, in the free end of the lower arm of the delamination crack (Fig. 1) by Eq. (25).

$$\varphi = \frac{u_{H1} - u_{H2}}{h_1} \tag{25}$$

where φ varies with time according to (1). The quantities, u_{H1} and u_{H2}, are presented via the strains by applying Eqs. (26) and (27), respectively.

$$u_{H1} = \varepsilon_{gr12} a + \varepsilon_{gr23}(l-a) \tag{26}$$

$$u_{H2} = \varepsilon_{dl12} a + \varepsilon_{dl23}(l-a) \tag{27}$$

where ε_{gr12} and ε_{gr23} are the strains at the upper surface of the lower arm of the delamination crack and along the line of the delamination in the intact portion, B_2B_3, of the beam, ε_{dl12} and ε_{dl23} are the strains at the lower surface of the beam in portions, B_1B_2 and B_2B_3, respectively, a and l are the lengths of the delamination crack and the beam structure, respectively (Fig. 1).

Eqs. (1), (25), (26) and (27) indicate that the change of the strains, ε_{gr12}, ε_{gr23}, ε_{dl12} and ε_{dl23}, with time can be written as given below.

$$\varepsilon_{gr12} = v_{gr12} t \tag{28}$$

$$\varepsilon_{gr23} = v_{gr23} t \tag{29}$$

$$\varepsilon_{dl12} = v_{dl12} t \tag{30}$$

$$\varepsilon_{dl23} = v_{dl23} t \tag{31}$$

where v_{gr12}, v_{gr23}, v_{dl12} and v_{dl23} are velocities of the strains. In order to determine these velocities, first, we write Eqs. (32) and (33) (these equations reflect the fact that the axial force in the lower arm of the delamination crack and the beam portion, B_2B_3, are zero).

$$N_{lwd} = 0 \tag{32}$$

$$N_{B2B3} = 0 \tag{33}$$

where the subscripts, lwd and B_2B_3, refer to the lower arm of the delamination crack and the intact portion of the beam, respectively. Eq. (34) reflects the fact that the bending moments on both sides of section, B_2, of beam structure are equal.

$$M_{lwd} = M_{B2B3}. \tag{34}$$

The axial forces and the bending moments involved in Eqs. (32)-(34) can be presented via the stresses in the layers of the lower arm of the delamination crack and beam portion, B_2B_3.

Therefore, Eqs. (32)-(34) are transformed as

$$N_{lwd} = b\sum_{i=1}^{i=m_{lwd}} \int_{z_{1i}}^{z_{1i+1}} \sigma_{lwdi} dz_1 = 0 \tag{35}$$

$$N_{B2B3} = b\sum_{i=1}^{i=m} \int_{z_{2i}}^{z_{2i+1}} \sigma_i dz_2 = 0 \tag{36}$$

$$b\sum_{i=1}^{i=m_{lwd}} \int_{z_{1i}}^{z_{1i+1}} \sigma_{lwdi} z_1 dz_1 = b\sum_{i=1}^{i=m} \int_{z_{2i}}^{z_{2i+1}} \sigma_i dz_2 \tag{37}$$

where b is the beam width. The stresses, σ_{lwdi} and σ_i, are functions of the strains, ε_{lwd} and ε, according to (2).

The distributions of strains, ε_{lwd} and ε, along h_1 and h are presented in terms of velocities, v_{gr12}, v_{dl12}, v_{gr23} and v_{dl23}, as written below, i.e.

$$\varepsilon_{lwd}(z_1) = \frac{v_{gr12}t + v_{dl12}t}{h_1}\left(\frac{h_1}{2} - z_1\right) - v_{dl12}t \tag{38}$$

$$\varepsilon(z_2) = \frac{v_{gr23}t + v_{dl23}t}{h_1}\left(\frac{h}{2} - z_2\right) - v_{dl23}t \tag{39}$$

where

$$-\frac{h_1}{2} \le z_1 \le \frac{h_1}{2} \tag{40}$$

$$-\frac{h}{2} \le z_2 \le \frac{h}{2} \tag{41}$$

Here h is the beam thickness. Finally, Eqs. (25), (35), (36) and (37) are solved by the MatLab for the unknown quantities, v_{gr12}, v_{gr23}, v_{dl12} and v_{dl23}, at various values of time. Then, σ_{lwdi}, σ_i, ε_{lwd} and ε are used in (10) and (11) for obtaining J_{D1} and J_{D2} (the integration is carried-out by the MatLab).

The correctness of the *J* integral analysis is proved here by deriving the SERR, G. The latter is defined by Eq. (42).

$$G = \frac{dU^*}{bda} \tag{42}$$

where U^* is the complementary strain energy in the beam structure under consideration.

U^* is determined as given below.

$$U^* = U^*_{lwd} + U^*_{B2B3} \tag{43}$$

where the subscripts, lwd and B_2B_3, refer to the lower arm of the delamination crack and the intact portion of the beam structure, respectively.

The quantities, U^*_{lwd} and U^*_{B2B3}, are obtained as written below.

$$U^*_{lwd} = ab\sum_{i=1}^{i=m_{lwd}} \int_{z_{1i}}^{z_{1i+1}} u^*_{0lwdi} dz_1 \tag{44}$$

$$U^*_{B2B3} = (l-a)b\sum_{i=1}^{i=m} \int_{z_{2i}}^{z_{2i+1}} u^*_{0i} dz_2 \tag{45}$$

where u^*_{0lwdi} and u^*_{0i} are the complementary strain energy densities. They are defined as given below.

$$u^*_{0lwdi} = \sigma_{lwdi}\varepsilon_{lwdi} - \int \sigma_{lwdi} d\varepsilon_{lwd} \tag{46}$$

$$u^*_{0i} = \sigma_i \varepsilon_i - \int \sigma_i d\varepsilon \tag{47}$$

Then, the SERR is found via (42). The integration is performed by the MatLab. Since the SERR matches the values of the integral *J,* it can be concluded that the analysis performed in this work is correct.

3. Application of the analysis

When a delamination crack is observed in an engineering structure during regular inspection, there are several questions which have to be answered in order to check if the further functioning of the structure is safe.

This issue is addressed here theoretically for the beam structure with a delamination crack shown in Fig. 1 by analyzing the integral *J* with the help of the approach developed in section 2 of the present work. The analysis is carried-out assuming that $l = 0.500$ m, $b = 0.010$ m, $h = 0.016$ m, $m = 5$, $m_{lwd} = 3$, $\lambda = 0.5$, $\mu = 0.5$, $\rho = 0.5$, $\dot{\varepsilon}_0 = 0.001$ 1/s, $E_{idl}/E_{igr} = 0.4$, $n_{idl}/n_{igr} = 0.4$ and $L_{idl}/L_{igr} = 0.4$ where $i = 1, 2, \ldots, 5$. In particular, three questions are considered here. The first question is about the external influence applied on the beam structure, i.e., what is the safe external influence under which the delamination crack will not begin to grow. The second question is about the safe length of the delamination crack, i.e., what is the maximum length under which delamination crack growth will not occur. The third question concerns the time-dependent behavior (this question is important since the external influence applied on the beam structure under consideration is time-dependent). In particular, it is determined after passing of what interval of time the delamination crack would begin to grow. Finally, it is analyzed what is the effect of introducing an additional support of the beam on the value of time at which the delamination crack growth would begin.

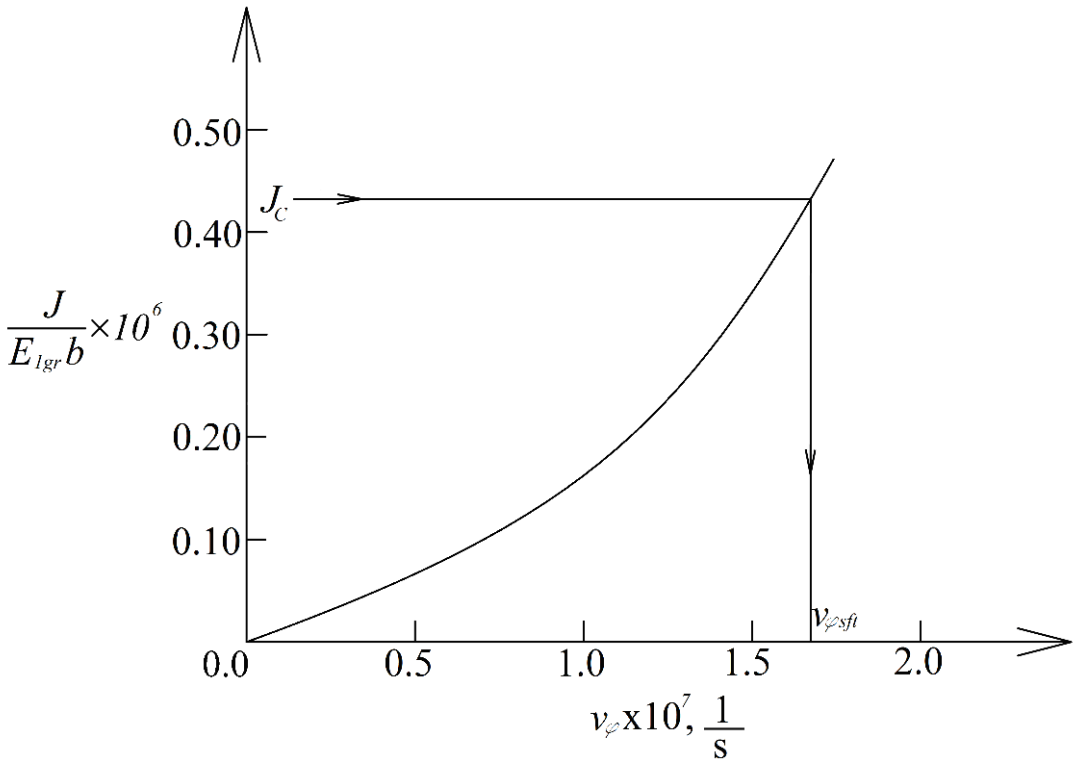

Fig. 4 Variation of the normalized *J* integral with v_φ

In order to determine the safe external influence on the beam, the *J* integral is shown as a function of the value of v_φ in Fig. 4. The *J* integral is expressed in normalized form by applying the Eq. $J/(E_{1gr}b)$ in Fig. 4.

The maximum safe value of v_φ is denoted by $v_{\varphi sft}$. This is the value at which the *J* integral becomes equal to the fracture toughness, J_C (the latter is a parameter defined as the *J* integral value at the onset of delamination crack growth). The value of $v_{\varphi sft}$ is presented in Table 1. For values of v_φ that are less than $v_{\varphi sft}$ the safe functioning of the beam structure is guaranteed in sense that the delamination crack will not begin to grow.

The treatment of the question for the safe length of the delamination crack is illustrated here by the graph reported in Fig. 5. This graph presents the normalized *J* integral as a function of the normalized delamination crack length (the latter is defined as a/l). The maximum safe length of the delamination crack is defined as the length that corresponds to J_C according to the graph in Fig. 5. The maximum safe length of the crack, a_{sft}, is shown in Table 1. If the delamination length is less than the maximum safe length according to the graph in Fig. 5 the crack growth will not occur and the beam structure can be used safely.

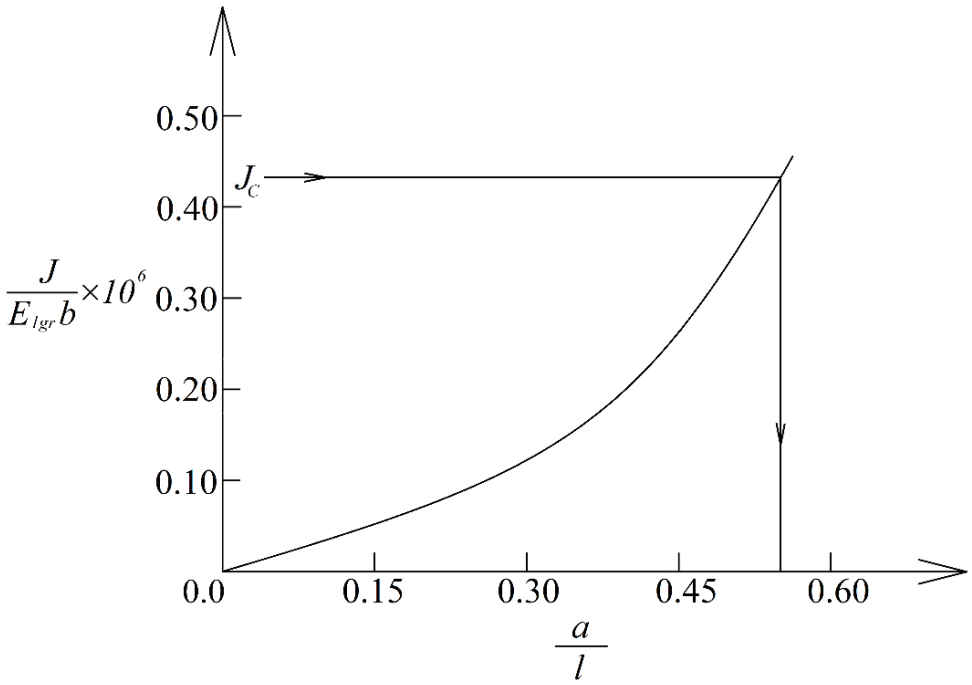

Fig. 5 Variation of the normalized J integral with a/l

Table 1 Values of various quantities determined by applying the approach based on the J integral

Quantity	$v_{\phi sft}$, 1/s	a_{sft}, m	t_0, s	t_1, s	t_2, s
Value	1.66 x 10^{-7}	0.27	132.5 x 10^3	244.0 x 10^3	349.0 x 10^3

The question for the safe functioning of the beam structure in terms of time is dealt with next. Determination of the interval of time after passing of which the delamination crack would begin to grow is illustrated with the help of the graph shown in Fig. 6. The time is presented along the abscissa in Fig. 6 in normalized form by using the formula t/t_{rfr} where t_{rfr} is a reference time ($t_{rfr}=1.8\times10^3$ s). The normalized J integral is presented along the abscissa (Fig. 6). The value of time, t_1, that corresponds to J_c is the time after passing of which the delamination crack growth would begin (Fig. 6). In this sense, the beam structure functioning is safe for time less than t_1. The value of t_1 is shown in Table 1.

The effect of introducing of an additional support of the beam on the value of time at which the delamination crack growth would begin is assessed next. For this purpose, it is assumed that at time value, $t_0=132.5\times10^3$ s, where $t_0<t_1$ two short horizontal rods are introduced on the free end of the upper arm of the delamination crack as can be seen in Fig. 7. In this way the beam is

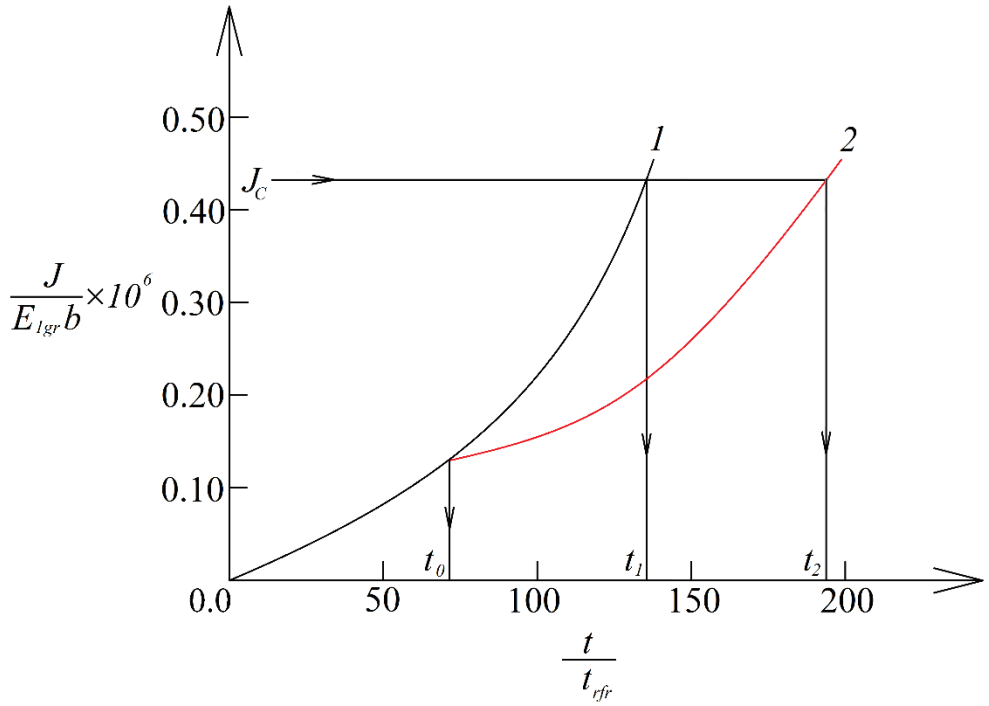

Fig. 6 Variation of the normalized J integral with normalized time (curve 1 – for beam without additional support, curve 2 – for beam with additional support)

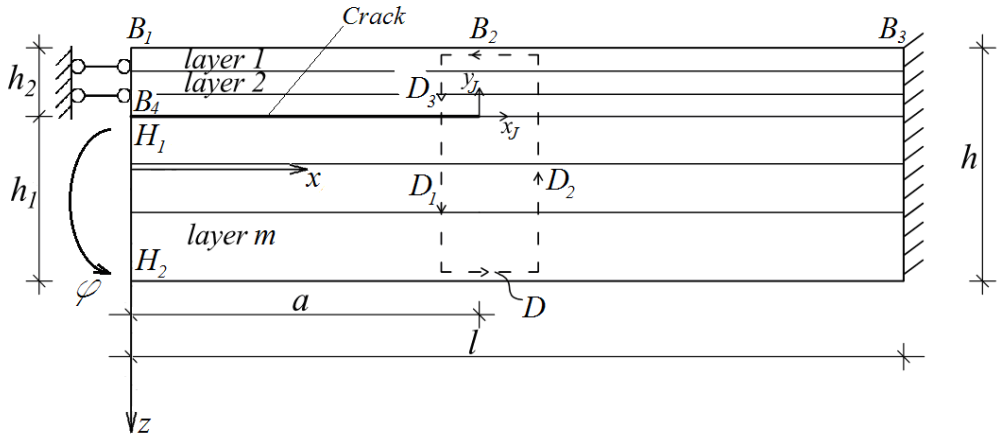

Fig. 7 Beam structure with additional support introduced in the free end of the delamination crack upper arm

transformed in a statically indeterminate structure. The delamination is studied by the integral J along the contour, D. The integral J solution is presented by the equation given below.

$$J_D = J_{D1} + J_{D2} + J_{D3} \tag{48}$$

Where J_{D1} and J_{D2} are expressed by using Eqs. (10) and (11), respectively. The subscript, D_2, refers to part, D_2, of the integration contour.

J_{D3} is written as given below.

$$J_{D3}= \sum_{i=1}^{i=m_{upd}} \int \left[u_{0D3i} \cos\alpha_{D3} - \left(p_{xJD3i} \frac{\partial u_{D3}}{\partial x_J} + p_{yJD3i} \frac{\partial v_{D3}}{\partial x_J} \right) \right] ds_3 \tag{49}$$

where m_{upd} is the number of layers in the upper arm of the delamination crack (the thickness of this arm is h_2).

The quantities involved in (49) are defined by Eqs. (50)-(55).

$$u_{0D3i} = \int \sigma_{updi} d\varepsilon_{upd} \tag{50}$$

$$\cos\alpha_{D3} = -1 \tag{51}$$

$$p_{xJD3i} = -\sigma_{updi} \tag{52}$$

$$\frac{\partial u_{D3}}{\partial x_J} = \varepsilon_{upd} \tag{53}$$

$$p_{yJD3i} = 0 \tag{54}$$

$$ds_3 = dz_3 \tag{55}$$

where

$$-\frac{h_2}{2} \le z_3 \le \frac{h_2}{2} \tag{56}$$

Here, σ_{updi} and ε_{upd} are the stress and strain in a layer of the upper arm of the delamination crack, z_3 is the vertical axis of the cross-section of the upper arm.

For analyzing the quantities involved in Eqs. (50)-(55), the mechanical response of the beam in Fig. 7 is studied. In order to account for the short horizontal rods introduced in the free end of the upper arm of the delamination crack, two additional equations are composed as follows:

$$u_{upd} = 0 \tag{57}$$

$$\varphi_{upd} = 0 \tag{58}$$

where u_{upd} and φ_{upd} are the axial displacement and the angle of rotation of the free end of the upper arm, respectively.

The quantities, u_{upd} and φ_{upd}, are presented by Eqs. (59) and (60), i.e.

$$u_{upd} = \frac{u_{B1} + u_{B4}}{2} \tag{59}$$

$$\varphi_{upd} = \frac{u_{B1} - u_{B4}}{h_2} \tag{60}$$

where u_{B1} and u_{B4} are the longitudinal displacements of points, B_1 and B_4, respectively.

These displacements are expressed by the equations given below, i.e.

$$u_{B1} = \varepsilon_{up12} a + \varepsilon_{up23}(l - a) \tag{61}$$

$$u_{H2} = \varepsilon_{lw12} a + \varepsilon_{gr23}(l - a) \tag{62}$$

where ε_{up12} and ε_{up23} are the strains at the upper surface of the upper arm of the delamination crack and the upper surface of the beam in its intact portion, ε_{lw12} is the strain at the lower surface of the upper arm of the delamination crack.

The change of the strains, ε_{up12}, ε_{up23} and ε_{lw12} with time can be expressed by the next three equations

$$\varepsilon_{up12} = v_{up12} t \tag{63}$$

$$\varepsilon_{up12} = v_{up12} t \tag{64}$$

$$\varepsilon_{lw12} = v_{lw12} t \tag{65}$$

The velocities, v_{up12}, v_{up23} and v_{lw12}, are unknown. For determining these velocities, first, we compose equilibrium Eqs. (66) and (67) for section, B_2, of the beam.

$$N_{upd} + N_{B2B3} = 0 \tag{66}$$

$$M_{lwd} + M_{upd} + M_{B2B3} = 0 \tag{67}$$

where N_{upd} and N_{B2B3} are the axial forces in the upper arm of the delamination crack and the intact portion of the beam, M_{upd} is the bending moment in the upper arm of the delamination crack.

The axial forces and the bending moments in Eqs. (66) and (67) are expressed via the stresses, σ_{updi}, σ_{lwdi} and σ_i, in the layers of the two delamination crack arms and the intact portion of the beam. In this way, Eqs. (66) and (67) are re-written as given below.

$$b \sum_{i=1}^{i=m_{upd}} \int_{z_{3i}}^{z_{3i+1}} \sigma_{updi} dz_3 + b \sum_{i=1}^{i=m} \int_{z_{2i}}^{z_{2i+1}} \sigma_i dz_2 = 0 \tag{68}$$

$$b \sum_{i=1}^{i=m_{lwd}} \int_{z_{1i}}^{z_{1i+1}} \sigma_{lwdi} z_1 dz_1 + b \sum_{i=1}^{i=m_{upd}} \int_{z_{3i}}^{z_{3i+1}} \sigma_{updi} z_3 dz_3 + b \sum_{i=1}^{i=m} \int_{z_{2i}}^{z_{2i+1}} \sigma_i z_2 dz_2 = 0 \tag{69}$$

The stresses, σ_{updi}, σ_{lwdi} and σ_i, are related to the strains, ε_{upd}, ε_{lwd} and ε, via the law (2).

The strain, ε_{upd}, in the upper arm of the delamination crack is distributed along h_2 as

$$\varepsilon_{upd}(z_3)=\frac{\nu_{up12}t+\nu_{lw12}t}{h_2}\left(\frac{h_2}{2}-z_3\right)-\nu_{lw12}t \tag{70}$$

where

$$-\frac{h_2}{2}\le z_3\le\frac{h_2}{2} \tag{71}$$

The distributions of ε_{lwd} and ε along h_1 and h are described by Eqs. (38) and (39), respectively.

Eqs. (25), (35), (67), (58), (68) and (69) are used for determining ν_{gr12}, ν_{dl12}, ν_{up12}, ν_{dl12}, ν_{up23} and ν_{lw12} by the MatLab. Then Eqs. (10), (11) and (48) are be applied for solving J_{D1}, J_{D2} and J_{D3} by the MatLab. Finally, the integral *J* is found by (48).

The *J* integral is verified by deriving the SERR for the delamination crack in the beam in Fig. 7. Eq. (42) is applied. The complementary strain energy is determined by the equation given below.

$$U^*=U^*_{lwd}+U^*_{B2B3}+U^*_{upd} \tag{72}$$

The quantities, U^*_{lwd} and U^*_{B2B3}, are obtained by (44) and (45), respectively. The complementary strain energy, U^*_{upd}, in the upper arm of the delamination crack is found by Eq. (73).

$$U^*_{upd}=ab\sum_{i=1}^{i=m_{upd}}\int_{z_{3i}}^{z_{3i+1}}u^*_{0updi}dz_3 \tag{73}$$

where

$$u^*_{0updi}=\sigma_{updi}\varepsilon_{updi}-\int\sigma_{updi}d\varepsilon_{upd}\,. \tag{74}$$

The so derived SERR matches the value of the integral *J* which proves the correctness of the current analysis.

The normalized *J* integral for the beam structure with additional support (refer to Fig. 7) is presented as a function the normalized time in Fig. 6 (the corresponding graph is drawn in red) for comparison with the graph for the beam structure without additional support (refer to Fig. 1). It is seen form Fig. 6 that the value of time, t_2, after passing of which the delamination crack in the beam with additional support would begin to grow is bigger than t_1 (the value of t_2 is shown in Table 1). This finding indicates that by introducing additional supports, the time of safe functioning of the beam can be prolonged.

4. Conclusions

It is demonstrated that the approach developed here can be applied for answering important questions about further safe functioning of a beam structure in which a delamination crack is observed through routine inspections. For instance, it is shown that the approach can be used for determining the maximum safe velocity of the angle of rotation of the free end of the lower arm of the delamination crack. The safe length of the delamination crack also is determined by the approach. Besides, the time of safe functioning of the beam is determined too (the time of safe functioning is defined as the interval of time after passing of which the delamination crack would begin to grow). Finally, an analysis of the effect of introducing an additional support in the beam on the time of safe functioning is carried-out. The additional support represents two short horizontal rods introduced at the free end of the upper arm of the delamination crack during lifetime. It is found that the additional support prolongs the time of safe functioning of the structure. The approach can be applied for treating various multilayered beam configurations with delamination crack (the beam configuration studied here serves mainly as an illustrative example for application of the approach). This work contributes for reducing the cost of repairs and increasing the serviceability of multilayered beam structures with delamination cracks.

References

Ahmed, R.A., Fenjan, R.M. and Faleh, N.M. (2019), "Analyzing post-buckling behavior of continuously graded FG nanobeams with geometrical imperfections", *Geomech. Eng.*, **17**(2), 175-180. https://doi.org/10.12989/gae.2019.17.2.175.

Akbaş, S.D., Dastjerdi, S., Akgöz, B. and Civalek, Ö. (2022), "Dynamic analysis of functionally graded porous microbeams under moving load", *Transport in Porous Media*, **142**(1-2), https://doi.org/10.1007/s11242-021-01686-z.

Akbaş, Ş.D., Ersoy, H., Akgöz, B. and Civalek, Ö. (2021), "Dynamic analysis of a fiber-reinforced composite beam under a moving load by the ritz method", *Mathematics*, **9**(9), 1048. https://doi.org/10.3390/math9091048.

Almeida, J.H.S., Souza, S.D.B., Botelho, E.C. and Amico, S.C. (2016), "Carbon fiber-reinforced epoxy filament-wound composite laminates exposed to hygrothermal conditioning", *J. Mater. Sci.*, **51**, 4697–4708. https://doi.org/10.1007/s10853-016-9787-9.

Boyano, A., Lopez-Guede, J.M., Torre-Tojal, L., Fernandez-Gamiz, U., Zulueta, E. and Mujika, F. (2021), "Delamination fracture behavior of unidirectional carbon reinforced composites applied to wind turbine blades", *Materials*, **14**(3), 593. https://doi.org/10.3390/ma14030593.

Broek, D. (1986), *Elementary engineering fracture mechanics*, Springer.

Butcher, R.J., Rousseau, C.E. and Tippur, H.V. (1999), "A functionally graded particulate composite: Measurements and failure analysis", *Acta. Mater.*, **47**(2), 259-268. https://doi.org/10.1016/S1359-6454(98)00305-X.

Cinefra, M. and Soave, M. (2011), "Accurate vibration analysis of multilayered plates made of functionally graded materials", *Mech. Adv. Mater. Struct.*, **18**(1), 3-13. https://doi.org/10.1080/15376494.2010.519204.

Civalek, Ö., Akbas, S.D., Akgöz, B. and Dastjerdi, S. (2021), "Forced vibration analysis of composite beams Reinforced by carbon nanotubes", *Nanomaterials*, **11**, 571. https://doi.org/10.3390/nano 11030571.

Dastjerdi, S., Akgöz, B., Civalek, Ö., Malikan, M. and Eremeyev, V.A. (2020), "On the non-linear dynamics of torus-shaped and cylindrical shell structures", *Int. J. Eng. Sci.*, **156**, 103371. https://doi.org/10.1016/j.ijengsci.2020.103371.

Dastjerdi, S., Alibakhshi, A., Akgöz, B. and Civalek, Ö. (2022), "A novel nonlinear elasticity approach for analysis of nonlinear and hyperelastic structures", *Eng. Anal. Bound. Elem*., **143**, 219-236. https://doi.org/10.1016/j.enganabound.2022.06.015.

Dastjerdi, S., Alibakhshi, A., Akgöz, B. and Civalek, Ö. (2023), "On a comprehensive analysis for mechanical problems of spherical structures", *Int. J. Eng. Sci.*, **183**, 103796. https://doi.org/10.1016/j.ijengsci.2022.103796.

Dinesh Babu, V., Arumugam, V. and Santulli, C. (2023), "Experimental investigation of the enhancement of delamination resistance in glass/epoxy curved laminates", *J. Mater. Sci*., **58**, 14723-14739. https://doi.org/10.1007/s10853-023-08954-x.

Dolgov, N.A. (2002), "Effect of the elastic modulus of a coating on the serviceability of the substrate-coating system", *Strength Mater.*, **37**(2), 422-431. https://doi.org/10.1007/s11223-005-0053-7.

Dolgov, N.A. (2005), "Determination of stresses in a two-layer coating", *Strength Mater.*, **37**(2), 422-431. https://doi.org/10.1007/s11223-005-0053-7.

Dolgov, N.A. (2016), "Analytical methods to determine the stress state in the substrate–coating system under mechanical loads", *Strength Mater.*, **48**(1), 658-667. https://doi.org/10.1007/s11223-016-9809-5.

Dowling, N.E. (2013), *Mechanical behaviour of materials*, Person.

Faleh, N.M., Ahmed, R.A. and Fenjan, R.M. (2018), "On vibrations of porous FG nanoshells", *Int. J. Eng. Sci.*, **133**, 1-14. https://doi.org/10.1016/j.ijengsci.2018.08.007.

Fenjan, R.M., Ahmed, R.A., Alasadi, A.A. and Faleh, N.M. (2019), "Nonlocal strain gradient thermal vibration analysis of doublecoupled metal foam plate system with uniform and non-uniform porosities", *Coupled Syst. Mech.*, **8**(3), 247-257. https://doi.org/10.12989/csm.2019.8.3.247.

Fenjan, R.M., Ahmed, R.A., Faleh, N.M. and Hani, F.M. (2020), "Dynamic response of size-dependent porous functionally graded beams under thermal and moving load using a numerical approach", *Struct. Monit. Maint.*, **7**(2), 69-84. https://doi.org/10.12989/smm.2020.7.2.069.

Gasik, M.M. (2010), "Functionally graded materials: bulk processing techniques", *Int. J. Mater. Product Technol.*, **39**(1-2), 20-29. https://doi.org/10.1504/IJMPT.2010.034257.

Hedia, H.S., Aldousari, S.M., Abdellatif, A.K. and Fouda, N.A. (2014), "New design of cemented stem using functionally graded materials *(FGM)*", *Biomed. Mater. Eng*., **24**(3), 1575-1588. https://doi.org/10.3233/BME-140962.

Hirai, T. and Chen, L. (1999), "Recent and prospective development of functionally graded materials in Japan", *Mater. Sci. Forum.*, **308-311**(4), 509-514. https://doi.org/10.4028/www.scientific.net/MSF.308-311.509.

Hofinger, I., Oechsner, M., Bahr, HA. and Swain, M.V. (1998), "Modified four-point bending specimen for determining the interface fracture energy for thin, brittle layers", *Int. J. Fracture*, **92**, 213-220. https://doi.org/10.1023/A:1007530932726.

Huang, T. and Bobyr, M. (2023), "A review of delamination damage of composite materials", *J. Compos. Sci.*, **7**(11), 468. https://doi.org/10.3390/jcs7110468.

Köllner, A., Jungnickel, R. and Völlmecke, C. (2016), "Delamination growth in buckled composite struts", *Int. J. Fract.*, **202**, 261-269. https://doi.org/10.1007/s10704-016-0158-y.

Kushnir, R.M., Yasinskyy, A.V. and Tokovyy, Y.V. (2022), "Effect of material properties in the direct and inverse thermomechanical analyses of multilayer functionally graded solids", *Adv. Eng. Mater*., **24**, 2100875. https://doi.org/10.1002/adem.202100875.

Liu, G.R., Han, X., Xu, Y.G. and Lam, K.Y. (2001), "Material characterization of functionally graded material by means of elastic waves and a progressive-learning neural network", *Compos. Sci. Technol.*, **61**(10), 1401-1411. https://doi.org/10.1016/S0266-3538(01)00033-1.

Long, V.T. and Tung, H.V. (2023), "Thermo-torsional buckling and postbuckling of thin FGM cylindrical shells with porosities and tangentially restrained edges, mechanics based design of structures and machines", **51**(12), 7056-7075. https://doi.org/10.1080/15397734.2022.2084752.

Mahamood, R.M. and Akinlabi, E.T. (2017), *Functionally Graded Materials*, Springer.

Markworth, A.J., Ramesh, K.S. and Parks, Jr. W.P. (1995), "Review: modeling studies applied to functionally graded materials", *J. Mater. Sci.*, **30**(3), 2183-2193. https://doi.org/10.1007/BF01184560.

Miyamoto, Y., Kaysser, W.A., Rabin, B.H., Kawasaki, A. and Ford, R.G. (1999), *Functionally Graded Materials: Design, Processing and Applications*, Kluwer Academic Publishers, Dordrecht/London/Boston.

Nemat-Allal, M.M., Ata, M.H., Bayoumi, M.R. and Khair-Eldeen, W. (2011), "Powder metallurgical fabrication and microstructural investigations of Aluminum/Steel functionally graded material", *Mater. Sci. Appl.*, **2**(5), 1708-1718. doi:10.4236/msa.2011.212228.

Rizov, V. (2020), "Influence of the viscoelastic material behaviour on the delamination in multilayered beam", *Procedia Struct. Integrity*, **25**, 88-100. https://doi.org/10.1016/j.prostr.2020.04.013.

Rizov, V.I. (2020), "Longitudinal fracture analysis of inhomogeneous beams with continuously changing radius of cross-section along the beam length", *Strength, Fract. Complexity Int. J.*, **13**(1), 31-43. https://doi.org/10.3233/SFC-200250

Rizov, V.I. (2023), "Delamination analysis of inhomogeneous viscoelastic beam of rectangular section subjected to torsion", *Coupled Syst. Mech.*, **12**(1), 69-81. https://doi.org/10.12989/csm.2023.12.1.069.

Rizov, V.I. (2024), "The effect of delamination between layers in U-shaped members made of functionally graded multilayered viscoelastic materials", *J. Appl. Comput. Mech.*, **10**, 830-841. https://doi.org/10.22055/jacm.2024.46014.4449.

Rizov, V.I. and Altenbach, H. (2022), "Multi-layered non-linear viscoelastic beams subjected to torsion at a constant speed: A delamination analysis", *Eng. Transactions*, **70**, 53-66. https://doi.org/10.24423/EngTrans.1720.20220303.

Rizov. V.I. (2014), "Delamination of multilayered viscoelastic inhomogeneous beams under moving loading", *Procedia Struct. Integrity*, **54**, 475-481. https://doi.org/10.1016/j.prostr.2024.01.109.

Rzeczkowski, J. (2021), "An experimental analysis of the end-notched flexure composite laminates beams with elastic couplings", *Continuum. Mech. Thermodyn.*, **33**, 2331-2343. https://doi.org/10.1007/s00161-020-00903-2.

Saiyathibrahim, A., Subramaniyan, R. and Dhanapl, P. (2016), "Centrefugally cast functionally graded materials – review", *Proceedings of the International Conference on Systems, Science, Control, Communications, Engineering and Technology*.

Shrikantha Rao, S. and Gangadharan, K.V. (2014), "Functionally graded composite materials: an overview", *Procedia Mater. Sci.*, **5**(1), 1291-1299. https://doi.org/10.1016/j.mspro.2014.07.442.

Sridhar, N., Massabò, R., Cox, B.N. and Beyerlein, I.J. (2002), "Delamination dynamics in through-thickness reinforced laminates with application to DCB specimen", *Int. J. Fracture*, **118**, 119-144. https://doi.org/10.1023/A:1022884410968.

Sy-NgocNguyen, JaehunLee, Jang-Woo Han, Maenghyo Cho (2020), "A coupled hygrothermo-mechanical viscoelastic analysis of multilayered composite plates for long-term creep behaviours", *Compos. Struct.*, **242**, 112030. https://doi.org/10.1016/j.compstruct.2020.112030**.**

Tokovyy, Y.V. (2023), "Elastic and thermoelastic response of multilayer inhomogeneous hollow cylinders", *Mech. Adv. Mater. Struct.*, **31**(17), 1-13. https://doi.org/10.1080/15376494.2023.2186548.

Treber, D., Haspel, B., Elsner, P. and Weidenmann, K.A. (2017), "Delamination fracture toughness of continuous glass-fiber/epoxy composites for structural applications", *Int. J. Plast. Technol.*, **21**, 39-54. https://doi.org/10.1007/s12588-016-9168-x.

Tsankov, T. (1996), *Theory of Plasticity*, Science.

Van Thinh, N. and Van Tung, H. (2023), "Free vibration and dynamical analyses of FGM plates with porosity and tangential edge constraints", *J. Vib. Eng. Technol.*, **12**, 5291–5305. https://doi.org/10.1007/s42417-023-01205-y.

Van Thinh, N. and Van Tung, H. (2023), "Nonlinear vibration of geometrically imperfect CNT-reinforced composite cylindrical panels exposed to thermal environments with elastically restrained edges", *Acta Mech.*, **235**, 1147-1164. https://doi.org/10.1007/s00707-023-03791-0.

Wu, X.L., Jiang, P., Chen, L., Zhang, J.F., Yuan, F.P. and Zhu, Y.T. (2014), "Synergetic strengthening by gradient structure", *Mater. Res. Lett.*, **2**(1), 185-191. https://doi.org/10.1080/21663831.2014.935821.